Separation Science and Technology
Publication details, including instructions for authors and subscription information:
http://www.informaworld.com/smpp/title~content=t713708471

A Model for Continuous Foam Concentration of Proteins: Effects of Kinetics of Adsorption of Proteins and Coalescence of Foam

Farooq Uraizee[a]; Ganesan Narsimhan[a]
[a] BIOCHEMICAL AND FOOD PROCESS ENGINEERING DEPARTMENT OF AGRICULTURAL ENGINEERING, PURDUE UNIVERSITY, WEST LAFAYETTE, INDIANA

To cite this Article Uraizee, Farooq and Narsimhan, Ganesan(1995) 'A Model for Continuous Foam Concentration of Proteins: Effects of Kinetics of Adsorption of Proteins and Coalescence of Foam', Separation Science and Technology, 30: 6, 847 — 881
To link to this Article: DOI: 10.1080/01496399508015404
URL: http://dx.doi.org/10.1080/01496399508015404

SEPARATION SCIENCE AND TECHNOLOGY, **30**(6), pp. 847–881, 1995

A Model for Continuous Foam Concentration of Proteins: Effects of Kinetics of Adsorption of Proteins and Coalescence of Foam

FAROOQ URAIZEE and GANESAN NARSIMHAN*
BIOCHEMICAL AND FOOD PROCESS ENGINEERING
DEPARTMENT OF AGRICULTURAL ENGINEERING
PURDUE UNIVERSITY
WEST LAFAYETTE, INDIANA 47907

ABSTRACT

A model for concentration of proteins from dilute solutions in a continuous foam fractionation column is proposed. This model accounts for (1) kinetics of adsorption of proteins in the liquid pool as well as in the foam, (2) liquid drainage from thin films due to Plateau border suction and disjoining pressure, (3) gravity drainage of liquid from Plateau borders, and (4) bubble coalescence in the foam. Protein enrichment and recovery were found to increase as the liquid pool height increased, eventually attaining constant values (corresponding to adsorption equilibrium), thus demonstrating the strong dependence of protein separation on adsorption kinetics. Higher enrichments and lower recoveries were obtained for smaller gas velocities, larger bubble sizes, and higher feed flow rates. Enrichments as well as recoveries were higher at lower feed concentrations. Coalescence was found to lead to higher enrichments and lower recoveries, this dependence being stronger for larger inlet bubble sizes.

Key Words. Foam fractionation; Foam concentration; Protein separation; Protein adsorption; Preconcentration of proteins

INTRODUCTION

Foam concentration is an adsorptive bubble separation technique in which soluble surface-active substances are concentrated from very dilute

* To whom correspondence should be addressed.

streams by preferential adsorption at the gas–liquid interface. The mixture of polar and nonpolar groups on the surface of a protein molecule renders them surface active, causing them to adsorb at the gas–liquid interface. This property makes foam concentration a viable technique for the concentration of proteins and enzymes. For a mixture of proteins in the solution, the more hydrophobic protein preferentially adsorbs at the surface of the gas bubble and hence a fractionation of proteins can be achieved. In such a situation, the operation is called foam fractionation. The most important features of foam concentration/fractionation compared to conventional separation techniques are its high separation efficiency and low capital and operating costs.

Various phenomena that take place in the foam column were discussed in detail by Narsimhan and Ruckenstein (1). Early efforts to model the behavior of a foam column were undertaken by Miles et al. (2) and Jacobi et al. (3). They predicted the foam density by assuming equal sized bubbles and by accounting only for the gravity drainage of the liquid from the Plateau borders. Hartland and Barber (4) predicted the liquid holdup profile in a foam column by considering the liquid drainage from the Plateau border as well as from thin films. They accounted for the variation of liquid holdup along the foam height but considered the walls of Plateau borders to be rigid. Steiner et al. (5) accounted for the variation of surface viscosity of the Plateau border walls through an adjustable parameter, but their results had poor agreement with the experimental observations. The assumption of rigid Plateau border walls was found to grossly underestimate the rate of liquid drainage (6). Desai and Kumar (7, 8) considered the Plateau borders as being triangular channels placed in nearly horizontal and nearly vertical orientations. The nearly vertical Plateau borders were assumed to receive liquid from the films as well as the nearly horizontal Plateau borders. On the other hand, the nearly horizontal Plateau borders receive liquid only from the films. Surface viscosity was accounted for in the evaluation of exit foam densities, though the effect of van der Waals interaction on the drainage of film was neglected. The change in bubble size distribution due to interbubble gas diffusion has been quantified by Lemlich (9), Monsalve and Schechter (10), Callaghan et al. (11), and Krotov (12). In spite of extensive studies on the stability of isolated thin liquid films, very few attempts (1, 13, 14) have been made to couple the hydrodynamics of the foam bed to the instability of thin films in order to predict coalescence and subsequent foam collapse. The effects of 1) bubble size distribution, 2) bubble coalescence as a result of the rupture of thin films caused by van der Waals forces mediated growth of thermal perturbations (1), and 3) interbubble gas diffusion have been accounted for in a comprehensive population balance model to simulate the perfor-

mance of a semibatch foam column for concentration of surfactants by Narsimhan and Ruckenstein (14). The simplifying assumption of equal sized bubbles has been shown to be valid for narrow inlet bubble size distributions, especially at higher superficial gas velocities and larger inlet bubble sizes (14). Brown et al. (15) developed a model for the hydrodynamics of a continuous foam fractionation column for the concentration of BSA (bovine serum albumin). The performance of this model was compared with the experimental results and it was found that the model compared qualitatively well with the experimental data. It was found that in order to make quantitative predictions of the experimental data, it was necessary to take into account the effect of coalescence of foam. These models assume adsorption equilibrium of the surface-active component at the gas–liquid interface. Such an assumption, though valid for small molecular weight surfactants, is inapplicable in the cases of proteins and enzymes because of their slow rates of adsorption.

In this paper we present a model for the concentration of proteins from dilute streams. The model presented here for the hydrodynamics of the foam column accounts for:

1. Kinetics of adsorption of protein in the liquid pool as well as in the foam
2. Drainage of liquid from thin films under the action of Plateau border suction and disjoining pressures due to van der Waals attraction and double layer repulsion
3. The gravity drainage of Plateau borders accounting for its surface viscosity
4. Surface pressure build up as a result of adsorption of proteins
5. Coalescence of foam

MODEL FOR CONTINUOUS FOAM CONCENTRATION OF PROTEINS

A schematic diagram of the foam concentration/fractionation column is shown in Fig. 1. A dilute protein stream is introduced at the bottom of the column, and a lean stream is withdrawn to maintain a constant liquid pool height. An inert gas is bubbled into the column through a capillary bundle located at the bottom of the column. Protein adsorbs onto the bubbles during the formation of bubbles and during their flight in the liquid pool. Upon reaching the top of the liquid pool, the bubbles form foam. Foam is continuously formed at the gas–liquid interface which moves up the column, entraining some of the liquid from the pool along with it. The foam from the top of the column is transferred to a foam breaker and

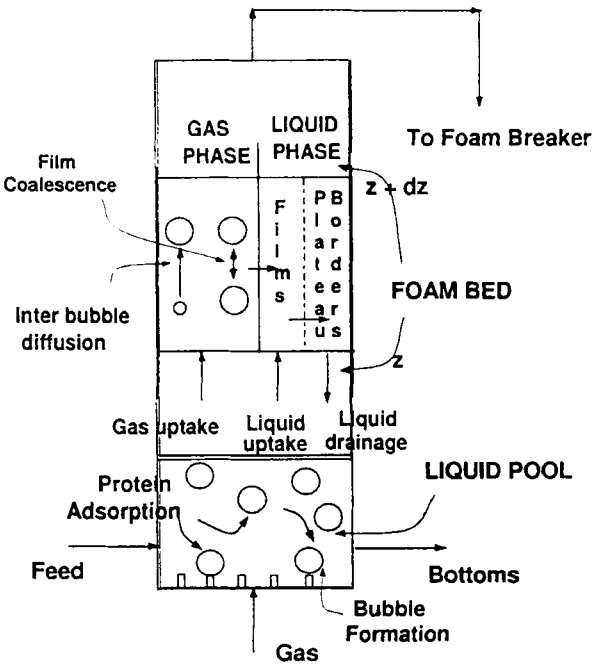

FIG. 1 Various phenomena that take place in the foam column.

collapsed to recover the proteins that are adsorbed onto the gas–liquid interface.

Various phenomena that take place in a foam column are also shown in detail in Fig. 1. Bubbles are formed at the tip of the capillary tube as the gas is sparged into the liquid pool. New surface is created continuously, and the bubble grows in size till it reaches its final size. At this stage the bubble detaches from the tip of the capillary tube and travels through the liquid pool. Protein adsorbs onto the bubble during its formation and its flight in the liquid pool. The rate of adsorption of protein depends on the rate of diffusion of protein molecules to the gas–liquid interface as well as the energy barrier (due to surface pressure and electric charge) that an adsorbing protein molecule has to overcome (16, 17). The extent of adsorption of protein at the interface is also influenced by the time of formation of the bubble and on its residence time in the liquid pool.

The foam bed consists of an assemblage of gas bubbles of different sizes separated by thin liquid films, thus creating a large gas–liquid interfacial

area. The entrained liquid is distributed between thin films and Plateau borders. As the foam moves through the bed, the liquid in the films drains into the neighboring Plateau borders under the action of Plateau border suction and disjoining pressure, and the liquid in the Plateau borders drains under gravity. Consequently, the liquid holdup decreases with foam height. In addition, the inert gas diffuses through thin films from smaller to larger bubbles because of the difference in their capillary pressure, thus resulting in the growth of larger bubbles at the expense of smaller ones. Proteins in solution exist as macro ions since they contain a large number of both acidic and basic sites, their net charge being dependent on the pH of the solution. Adsorption of these macro ions causes the gas–liquid interface to be charged, leading to double layer repulsion between the two approaching charged interfaces of the thin liquid film. As the film thickness becomes of the order of a thousand angstroms because of drainage, the disjoining pressure due to van der Waals attraction and double layer repulsion may counterbalance the Plateau border suction, after which the film reaches an equilibrium thickness. The subsequent behavior of this equilibrium film will be influenced greatly by the thermal and mechanical interfacial disturbances to which it is subjected. The rupture of these films leads to the coalescence of neighboring bubbles.

The foam from the top of the foam column is transferred to a foam breaker. The top product obtained by breaking the foam is enriched in protein because of the recovery of adsorbed protein from the large gas–liquid interfacial area. The performance of the foam concentration column depends on factors such as gas velocity, bubble size, pool and foam heights, concentration and flow rate of feed, kinetics of adsorption of proteins, pH and ionic strength of the solution, the bubble coalescence and the bubble size distribution, as well as the mode of operation.

Two important measures of the performance of a foam column are enrichment e_n and recovery R_r, and are given by

$$e_n = c_T/c_F \tag{1}$$

and

$$R_r = \frac{c_T F_t}{c_F F} = e_n \frac{F_t}{F} \tag{2}$$

(see the Symbols Section at the end of the text). It is desirable to design a foam concentration column such that the enrichment and recovery are high. To evaluate the enrichment and recovery of the protein in the foam column, it is necessary to know the flow rate and protein concentration of the top product. The liquid that emerges as the top product comes from the liquid that is present in the films and in the Plateau borders. The

protein in the top product comes from 1) the bulk liquid in the films and the Plateau borders, and 2) protein adsorbed at the gas–liquid interface. It is therefore necessary to evaluate the amount of liquid in the thin films and Plateau borders and the bulk and surface concentration of protein at the top of the foam column in order to predict enrichment and recovery. Profiles of liquid holdup, bulk, and surface concentrations exist along the height of the foam column as a result of liquid drainage and protein adsorption. Consequently, balance equations for liquid and protein have to be solved in order to predict these profiles.

Structure of the Foam Bed

Because of low liquid holdup, the gas bubbles in a foam are deformed and assume the shape of pentagonal dodecahedrons (7, 14). The faces of adjacent bubbles form films, and the films intersect in Plateau borders. The coordination number for the dodecahedral shape is 12, thus there are 12 bubbles surrounding a gas bubble, and hence the number of films per bubble, n_f, is 6. Three liquid films intersect to form a Plateau border. The number of Plateau borders per bubble, n_p, is 10, and the number of Plateau borders per bubble on a horizontal plane, n_p', is 2 ($= n_p/5$).

Balance Equations in the Foam

The following assumptions were employed in the development of the model for continuous foam concentration column:

1. Bubbles of the same size are sparged into the liquid pool.
2. There is negligible coalescence of bubbles during their travel through the liquid pool so that the foam at the foam–liquid interface consists of bubbles of the same size.
3. Coalescence in the foam leads to an increase in the bubble size along the axial distance in the foam, though the bubbles at any given cross section of the foam bed are of the same size.
4. The foam bed moves in a plug flow.
5. Liquid in the pool is well mixed.
6. The Plateau borders are randomly oriented.
7. Since the surface area of Plateau borders is very small compared to the surface area of films, the amount of protein adsorbed in them is neglected.
8. Protein adsorption in the thin film is mainly due to diffusion.

The total amount of liquid in the film per unit volume of the foam is $Nn_fA_fx_f$ whereas the amount of protein in the film per unit volume of the

foam is $Nn_fA_fx_fc_f + Nn_fA_f\Gamma$. Similarly, the amount of liquid and protein in the Plateau borders are given by Na_pn_pl and $Na_pn_plc_p$, respectively.

The liquid holdup in the foam bed, which is the fraction of volume of the foam bed occupied by liquid, at any location is therefore given by

$$\epsilon = Nn_fA_fx_f + Na_pn_pl \tag{3}$$

The concentration of the top product is obtained by

$$c_T = \frac{Nn_fA_fx_fc_f + Nn_pa_pc_pl + Nn_fA_f\Gamma}{\epsilon_T} \tag{4}$$

The number of bubbles per unit volume of the foam is related to the liquid holdup and the volume of a bubble, v_b, via

$$N = \frac{1 - \epsilon}{v_b} \tag{5}$$

For the evaluation of recovery, it is necessary to know the flow rate of the top product which is given by

$$F_t = \frac{G\epsilon_T}{1 - \epsilon_T} \tag{6}$$

Balance for Number of Bubbles

As the bubbles are generated from a capillary bundle, they are extremely uniform in size. Hence, the bubble size distribution at the foam–liquid interface is extremely narrow. The size of bubbles formed depends on the capillary diameter, surface tension, viscosity, density, and gas flow rate, and it is discussed in detail by Kumar and Kuloor (18). As the coalescence of bubbles depends on the film thickness, and the film thickness is more or less the same at any axial distance in the foam column, the coalescence frequency β is likely to be more or less constant at any cross section of the foam column.

Consider a section of the foam bed between z and $z + \Delta z$ as shown in Fig. 1. A balance of bubbles in the volume element is given by

$$\frac{d\eta}{dz} = -\beta \frac{N}{2} \tag{7}$$

where β, the coalescence frequency, is the fraction of bubbles coalescing per unit time, and η, the number of bubbles that flow per unit area in unit time in the foam, is given by

$$\eta = G/v_b \tag{8}$$

Since $v_b = 4\pi R^3/3$, combining Eqs. (5) and (8) with (7), we can write

$$\frac{dR}{dz} = \frac{\beta(1 - \epsilon)R}{6G} \tag{9}$$

The above equation relates the coarsening of the bubble size in the foam bed to the coalescence frequency.

Balance Equations for the Film

As the foam moves up (Fig. 1), the liquid from the films drains into the neighboring Plateau borders due to Plateau border suction, protein adsorbs onto the gas–liquid interface from the bulk, and there is coalescence of bubbles in the foam as a result of rupture of thin films leading to an increase in the bubble size. The liquid in the ruptured thin film is refluxed into the Plateau borders. The mass balance of liquid in the film is given by

$$-\frac{d}{dz}(\eta n_f A_f x_f) - NA_f n_f V_f - \frac{N}{2} n_f A_f x_f \beta = 0 \tag{10}$$

where V_f is the velocity of film drainage. In the above equation, the first term represents the change in volume of liquid in the films due to convection, the second term is the change in volume of liquid in the films due to drainage, and the third term represents the volumetric loss of liquid due to rupture of films.

Similarly, a balance equation for protein in thin films is given by

$$-\frac{d}{dz}[\eta n_f A_f x_f c_f] - NA_f n_f V_f c_f - \frac{N}{2} n_f A_f x_f \beta c_f - NA_f n_f \beta \left(\frac{d\Gamma}{dt}\right)_f = 0 \tag{11}$$

where $(d\Gamma/dt)_f$ is the rate of protein adsorption in the film. From Eqs. (10) and (11) we get

$$-\eta n_f A_f x_f \frac{dc_f}{dz} - Nn_f A_f \left(\frac{d\Gamma}{dt}\right)_f = 0 \tag{11a}$$

In order to solve the balance Eqs. (10) and (11a), we need to know V_f and $(d\Gamma/dt)_f$. Evaluation of these quantities is discussed below.

Velocity of Film Drainage

As pointed out earlier, the liquid from the films drains into the neighboring Plateau borders because of Plateau border suction. The driving force

ΔP responsible for the film drainage is given by

$$\Delta P = \frac{\sigma}{R_p} + \Pi_{vw} + \Pi_{DL} \tag{12}$$

where Π_{vw} and Π_{DL} refer to the disjoining pressures due to van der Waals and electrostatic interactions, respectively. The first term on the right-hand side is the Plateau border suction. The disjoining pressure becomes important only when the thickness of a draining thin film becomes of the order of a few hundred angstroms or smaller. The surface tension σ is given by

$$\sigma = \sigma_0 - \pi_s \tag{13}$$

The surface tension was evaluated at various surface concentrations of BSA using the surface equation of state (19).

The radius of curvature of the Plateau border, R_p, can be related geometrically to the film thickness and the cross-sectional area of the Plateau border to give (20)

$$R_P = \frac{-1.732x_f + [(1.732x_f)^2 - 0.644(0.433x_f^2 - a_p)]^{1/2}}{0.322} \tag{14}$$

The retarded van der Waals interaction between the approaching films is evaluated in terms of film thickness and the characteristic wavelength of interaction for water (21).

Adsorption of charged protein molecules on the thin films sets up an electrical double layer in the vicinity of the films. The overlap of electrical double layers of two films results in repulsive forces between them. The resulting disjoining pressure is evaluated in terms of film thickness and the surface charge density on the film (22). In order to evaluate the charge density on the surface of the film, it is necessary to know the number concentration of proteins at the interface.

The velocity of drainage of thin films can be evaluated by solving the equation of continuity and Navier–Stokes equation with appropriate boundary conditions. Denoting by R_F the radius of the circular film, $z' = 0$ the midplane of the plane parallel film, v_z and v_r the axial and radial components of the velocity, respectively, $\bar{\Gamma}$ the average surface concentration of protein at the film interface, and imposing the lubrication approximation, the simplified Navier–Stokes equation in dimensionless form reduces to

$$\frac{\partial^2 v_r^*}{\partial z^{*2}} = \frac{\partial p^*}{\partial r^*} \tag{15}$$

$$\partial p^*/\partial z^* = 0 \tag{16}$$

and the continuity equation

$$\frac{\partial v_z^*}{\partial z^*} + \frac{1}{r^*}\frac{\partial}{\partial r^*}(r^* v_r^*) = 0 \tag{17}$$

with the following boundary conditions:

$$\partial v_z^*/\partial z^* = 0 \qquad \text{at } z^* = 0 \tag{18}$$

$$v_z^* = -V^*/2 \qquad \text{at } z^* = 1/2 \tag{19}$$

$$\partial v_z^*/\partial z^* = 0 \qquad \text{at } z^* = 0 \tag{20}$$

$$S\gamma_f \frac{\partial v_r^*}{\partial z^*} = -\gamma_f \frac{\partial \Gamma^*}{\partial r^*} + S\frac{\partial}{\partial r^*}\left(\frac{1}{r^*}\frac{\partial}{\partial r^*}(r^* v_r^*)\right) \qquad \text{at } z^* = \frac{1}{2} \tag{21}$$

and

$$p^* = p_\delta^* \qquad \text{at } r^* = 1 \tag{22}$$

Equation (21) is the force balance at the film interface. γ_f is the inverse dimensionless surface viscosity and S is the ratio of the pressure drop responsible for film drainage and the surface pressure gradient, $(\partial\pi_s/\partial\Gamma)_{\bar{\Gamma}}$, evaluated at the average surface concentration $\bar{\Gamma}$. Since μ_s and π_s both depend on Γ, the dimensionless groups γ_f and S both vary with time because of adsorption of protein during film drainage. Consequently, the film drainage equations should strictly be solved along with the equations for the kinetics of protein adsorption in thin films. However, these equations can be decoupled by invoking certain simplifying assumptions. Except for very low feed concentrations and very small residence times of bubbles in the liquid pool, adsorption of protein onto the gas–liquid interface during the flight of the bubbles in the liquid pool would result in surface concentrations of protein close to monolayer coverage.† Consequently, the force due to the surface tension gradient $(-\partial\pi_s/\partial\Gamma)$ will be small, i.e., S will be large. The surface viscosity of interfacial protein layer can be evaluated from (23)

$$\mu_s = \frac{h}{A_F}\exp\left(\frac{\Delta G}{kT}\right)\exp\left(\frac{\pi_s A_F}{kT}\right) \tag{23}$$

For globular proteins such as bovine serum albumin, the surface viscosity of the interfacial adsorbed layer is sufficiently large. For example, the surface viscosity of the interfacial protein layer in equilibrium with a bulk concentration of 10^{-4} wt% is 60 mN·s/m (24). For a typical film thickness

† For example, for bovine serum albumin, the monolayer coverage is 2.85×10^{-6} kg/m^2, which is the equilibrium surface concentration for a bulk concentration of 10^{-3} wt% (24).

of 5×10^{-6} m and a typical bubble size of 1.0×10^{-3} m, the inverse dimensionless surface viscosity $\gamma_f = 4 \times 10^{-4}$. For higher surface concentrations normally encountered in foam columns, the surface viscosity will be higher, thus making γ_f even smaller. As a result, Eq. (21) reduces to

$$\frac{\partial}{\partial r^*}\left(\frac{1}{r^*}\frac{\partial}{\partial r^*}(r^* v_r^*)\right) = 0 \qquad \text{at } z^* = \frac{1}{2} \tag{21a}$$

It is to be noted that the above boundary condition does not involve the protein surface concentration. From (15), one obtains

$$v_r^* = \frac{1}{2}\left(\frac{\partial p^*}{\partial r^*}\right) z^{*2} + B(r^*) \tag{24}$$

where B is the unknown function. From Eqs. (17) and (24), one gets

$$\frac{\partial v_z^*}{\partial z^*} = -\frac{1}{r^*}\frac{\partial}{\partial r^*}\left[\frac{r^*}{2}\left(\frac{\partial p^*}{\partial r^*}\right) z^{*2} + r^* B\right]$$

Integrating the above equation and employing the boundary condition (20), one obtains

$$(\partial p^*/\partial r^*) = 12(v^* r^* - 2B) \tag{25}$$

Recognizing that the gas–liquid interface will be immobile for small inverse dimensionless surface viscosity and combining Eqs. (24), (25), and (21a) in the force balance,

$$F^* = 2\pi \int_0^1 p^* r^* dr^* = \pi(p_0^* + 1) \tag{26}$$

yields the Reynolds equation

$$V^* = 2/3 \tag{27}$$

or

$$V_f = \frac{2}{3}\frac{\Delta P x_f^3}{\mu R_F^2} \tag{27a}$$

for film drainage.

Protein Adsorption in Thin Films

As the foam moves up the column, protein from the film is adsorbed onto the gas–liquid interface by diffusion. Further, the film continues to thin as a result of film drainage. Protein balance at the gas–liquid interface

of a thin film is given by

$$\frac{\partial \Gamma}{\partial t} + \frac{1}{r}\frac{\partial}{\partial r}(r v_{rs}\Gamma) = -D\frac{\partial c_f}{\partial z} \qquad \text{at } z = x_f/2 \tag{28}$$

Since the interfacial mobility is negligible because of sufficiently high surface viscosity of an interfacial adsorbed layer of globular proteins, the above equation reduces to

$$\frac{\partial \Gamma}{\partial t} = -D\frac{\partial c_f}{\partial z} \qquad \text{at } z = \frac{x_f}{2} \tag{28a}$$

The protein concentration profile within the thin film can be evaluated from the solution of the continuity equation.

$$\frac{\partial c_f}{\partial t} + v_r\frac{\partial c_f}{\partial r} + v_z\frac{\partial c_f}{\partial z} = D\frac{\partial^2 c_f}{\partial z^2} + \frac{D}{r}\frac{\partial}{\partial r}\left(r\frac{\partial c_f}{\partial r}\right) \tag{29}$$

with the initial condition

$$\begin{aligned} t = 0, \qquad & c_f = c_{pool} \ \forall\ z \\ & \Gamma = \Gamma_0 \end{aligned} \tag{30}$$

The protein concentration in the thin films at the time of foam formation (or foam–liquid interface) can be taken to be uniform and equal to the pool concentration c_{pool}. In Eq. (30), Γ_0 is the surface concentration of protein at the foam–liquid interface. The boundary conditions are given by

$$c_f = c_s \qquad \text{at } z = x_f/2 \tag{31}$$

$$\partial c_f/\partial z = 0 \qquad \text{at } z = 0 \tag{32}$$

In Eq. (31), c_s is the subsurface protein concentration in equilibrium with the surface concentration of proteins and is evaluated using the adsorption isotherm proposed by Guzman et al. (16). The second boundary condition arises from symmetry of the concentration profile about the x-axis.

Equation (29) can be simplified by retaining only the dominant gradients to give

$$\frac{\partial c_f}{\partial t} + v_z\frac{\partial c_f}{\partial z} = D\frac{\partial^2 c_f}{\partial z^2} \tag{29a}$$

The protein continuity equation can be recast in terms of dimensionless quantities as

$$\frac{\partial c^*}{\partial t^*} + v_z^*\frac{\partial c^*}{\partial z^*} = \frac{1}{\mathrm{Pe}}\frac{\partial^2 c^*}{\partial z^{*2}} \tag{33}$$

where the Peclet number, $Pe = V_f x_f/D$, is the ratio of the time scales of diffusion and film drainage. The convective term can be neglected since the velocity of film drainage is small, i.e.,

$$\frac{\partial c^*}{\partial t^*} = \frac{1}{Pe}\frac{\partial^2 c^*}{\partial z^{*2}} \tag{33a}$$

For thick films near the foam–liquid interface, $Pe \gg 1$, so that negligible protein adsorption occurs during film drainage, i.e.,

$$\frac{\partial c^*}{\partial t^*} = \frac{1}{Pe}\frac{\partial^2 c^*}{\partial z^{*2}} \simeq 0 \tag{34}$$

which implies that

$$c^* = 1 \; \forall \; z^*$$

i.e., $dc^*/dz^* \simeq 0$. Therefore, $d\Gamma^*/dt^* = 0$, i.e., $\Gamma = \Gamma_0$.

On the other hand, as the film is draining, Pe decreases dramatically since the time scale of film drainage is a strong function of film thickness. For sufficiently thin films, therefore,

$$\frac{\partial c^*}{\partial t^*} = \frac{1}{Pe}\frac{\partial^2 c^*}{\partial z^{*2}} \tag{35}$$

which is obtained from Eq. (33) by neglecting the inertial terms. Since the film drainage rate is much smaller than the rate of protein adsorption, the film thickness can be considered constant. Equation (28a) can be recast in terms of dimensionless variables as

$$\frac{d\Gamma^*}{dt^*} = -\left(\frac{Dc_{pool}}{\Gamma_0 V_f}\right)\frac{\partial c^*}{\partial z^*} \qquad \text{at } z^* = \frac{1}{2} \tag{36}$$

Equations (35) and (36) are to be solved with the initial and boundary conditions

$$\begin{gathered} t^* = 0 \qquad c^* = 1 \; \forall \; z^*, \qquad \Gamma^* = 1 \\ z^* = 1/2, \qquad c^* = c_s^* = c_s/c_{pool} \\ z^* = 0, \qquad \partial c^*/\partial z^* = 0 \end{gathered} \tag{37}$$

to update the surface concentration of protein at the film interface.

Balance Equations in the Plateau Borders

Apart from the films, the foam bed contains Plateau borders which carry liquid along with them. As the foam moves up the column, the liquid from the films drains into the Plateau borders and the liquid in Plateau borders

drains into the liquid pool through the interconnected network of Plateau borders. In order to evaluate the rate of drainage of liquid from Plateau borders, the total cross section of the Plateau borders at a given height of the column must be calculated. Taking the mass balance on liquid in the Plateau borders between the distance z and $z + \Delta z$, we get (1, 15)

$$-\frac{d}{dz}(\eta a_p n_p l) + \frac{4}{15}\frac{d}{dz}(N n_p a_p u R) + N n_F A_f V_f + \frac{N}{2}\beta n_f A_f x_f = 0 \tag{38}$$

In the above equation, the first term represents the change in volume due to convection, the second term represents the change in volume due to gravity drainage, the third term represents the change in volume due to drainage of films to the Plateau borders, and the fourth term represents the volume of liquid that is added to the Plateau borders as a result of coalescence of films. The material balance of protein in the Plateau borders yields

$$-\frac{d}{dz}(\eta n_p a_p l c_p) + \frac{d}{dz}\left(\frac{4}{15} N n_p a_p u R c_p\right) + N n_f A_f V_f c_f + \frac{N}{2}\beta n_f A_f x_f c_f + \frac{N}{2}\beta n_f A_f \Gamma = 0 \tag{39}$$

Here the first term is the change in total protein due to convection, the second term is the change in total protein due to Plateau border drainage, and the third term arises from the protein entering the Plateau borders as a result of drainage of films. The last two terms arise from the addition of protein to the Plateau borders as a result of coalescence of films. In the above equation, the protein that is adsorbed in the Plateau borders is neglected since the surface area of Plateau borders is very small compared to that of film. This is not likely to introduce any serious error in the computation of enrichment as most of the adsorbed protein comes from the films. The average velocity of gravity drainage for a vertical Plateau border is obtained by solving the Navier–Stokes equation with appropriate boundary conditions and is given by (7)

$$u = \frac{c_v a_p \rho g}{20\sqrt{3}\mu} \tag{40}$$

where c_v is the velocity coefficient and is defined as the ratio of the average velocity of Plateau border drainage under given conditions to the average velocity of Plateau border drainage for infinite surface viscosity. The velocity coefficient is a function of inverse dimensionless surface viscosity and is evaluated using the expression given by Desai and Kumar (7).

Boundary Conditions

It is necessary to know the inlet parameters in order to solve Eqs. (7), (10), (11a), (38), and (39). Operating parameters such as the feed concentration, the flow rates, and the gas velocity are known. The coalescence frequency β of bubbles in the foam can be independently evaluated from the measurement of bubble size distribution along the length of the foam column. From knowledge of the size and the type of sparger, inlet bubble size is predicted using equations given elsewhere (25). It is difficult to predict the liquid holdup at the foam–liquid interface from the hydrodynamics of foam. Consequently, it is reasonable to assume that the gas bubbles at the foam–liquid interface are arranged as close packed spheres (1), therefore,

$$\epsilon_0 = N_0 n_f A_{f0} x_{f0} + N_0 a_{p0} n_p l_0 = 0.26 \tag{41}$$

Since there is no bubble coalescence in the liquid pool, the size of bubbles in the liquid pool and the gas–liquid interface are the same:

$$R = R_0 \tag{42}$$

A material balance around the foam bed yields

$$\frac{G\epsilon_0}{1 - \epsilon_0} = \frac{4}{15} N_0 n_p a_{p0} R_0 u_0 + \frac{G\epsilon_T}{1 - \epsilon_T} \tag{43}$$

where the subscript 0 refers to the quantities at the foam–liquid interface. The left term in the above equation is the rate of entrainment of liquid in the foam at the foam–liquid interface. The first term on the right-hand side is the rate of gravity drainage at the foam–pool interface and the second term is the top product flow rate. From the overall material balance for the liquid in the foam, the difference between the rates of uptake and drainage of liquid at the foam–liquid interface should be equal to the flow rate at the top of the foam column. The flow rates at the top of the foam column are usually much smaller than those at the foam–liquid interface because the liquid holdup at the top of the foam column is much smaller than 0.26 (1, 7). Consequently, one can approximate the rate of uptake at the foam–liquid interface as equal to the rate of drainage. Hence Eq. (43) reduces to

$$\frac{G\epsilon_0}{1 - \epsilon_0} = \frac{4}{15} N_0 n_p a_{p0} R u_0 \tag{44}$$

The area of the Plateau borders and the film thickness is related to Φ_{f0},

the fraction of liquid present in the film, by

$$a_{p0} = \frac{(1 - \Phi_{F0})\epsilon_0}{N_0 n_p l_0} \tag{45}$$

$$x_{f0} = \frac{\epsilon_0 \Phi_{F0}}{n_f N_0 A_{F0}} \tag{46}$$

and

$$N_0 = \frac{(1 - \epsilon_0)}{(4/3)\pi R_0^3} \tag{47}$$

In order to obtain the initial film thickness and the area of Plateau borders at the foam liquid interface, Eqs. (43) to (47) are to be solved with the constraint that $R_{p0} \geq 0$, where

$$R_{p0} = \frac{-1.732x_{f0} + [(1.732x_{f0})^2 - 0.644(0.433x_{f0}^2 - a_{p0})]^{1/2}}{0.322} \tag{48}$$

Further, the bulk concentration of protein in the film and the Plateau borders can, at the foam–liquid interface, be taken to be equal to the pool concentration.

$$c_f = c_p = c_{pool} \tag{49}$$

The surface concentration of protein at the film interface just above the liquid pool is equal to the surface concentration of protein for the bubble at the top of the liquid pool.

$$\Gamma = \Gamma_{pool} \tag{50}$$

The concentration Γ_{pool} is the result of protein adsorption onto the bubble during its formation and flight in the liquid pool. Hence

$$\Gamma_{pool} = \Gamma_{formation} + \int_0^{\theta} \left(\frac{d\Gamma}{dt}\right)_{pool} dt \tag{51}$$

where θ is the residence time of a bubble in the liquid pool and $(d\Gamma/dt)_{pool}$ is the rate of adsorption of protein onto the bubble surface in the liquid pool.

The protein adsorbed onto the bubble during formation depends upon its time of formation. It is postulated that the formation of the bubble takes place in two stages. In the first stage, known as the expansion stage, the bubble grows in size while remaining attached to the tip of the capillary tube. In the second stage, the bubble moves away from the capillary tube

and grows in size while being attached to the the capillary tip through a "neck." The complete detachment of the bubble from the capillary takes place when the length of the neck becomes equal to the bubble radius. The size of the bubble depends on the densities of the gas and the liquid, the interfacial tension, the capillary diameter, the gas flow rate, the height of the liquid column above the capillary, and pressure, and it is evaluated using equations given elsewhere (25).

During the formation of bubbles, protein is being adsorbed at the bubble surface. In addition, new surface is being created as the bubble expands. Accounting for the change in area with time and solving for the rate of diffusion-controlled adsorption of proteins at the bubble interface during its formation, one obtains (26)

$$\left(\frac{d\Gamma}{dt}\right)_{\text{formation}} = \frac{1}{2}\left(\frac{2.5484\ \dfrac{16\pi}{6}\left(\dfrac{3}{4\pi}\right)^{7/6} Q_f^{2/3} c_b}{\pi d_f^2 t_{\text{formation}}^{2/3}}\right)\sqrt{\frac{D}{t}} \tag{52}$$

In order to evaluate the second term on the right-hand side of Eq. (51), it is necessary to know θ, the residence time of a bubble in the liquid pool. The velocity of a bubble rising in the liquid pool is evaluated by equating the drag force on the bubble with the buoyancy force acting on the bubble:

$$\frac{A_p u_{\text{pool}}^2 \rho C_D}{2} = g\Delta\rho\,\frac{4}{3}\pi R^3 \tag{53}$$

The drag coefficients C_D are evaluated from correlations given elsewhere (27). The residence time of bubbles in the liquid pool is given by

$$\theta = L_{\text{pool}}/u_{\text{pool}} \tag{54}$$

A two-layer model proposed by Guzman et al. (16) is employed for the kinetics of protein adosorption, and it is given by

$$\frac{d\Gamma}{dt} = \frac{d\Gamma_1}{dt} + \frac{d\Gamma_2}{dt} \tag{55}$$

where

$$\frac{d\Gamma_2}{dt} = K_2\hat{a}\left(c_s\frac{d\Gamma_1}{dt} + \Gamma_1\frac{dc_s}{dt}\right)$$

$$\frac{dc_s}{dt} = \frac{c_s[1 + \lambda\Gamma_1(1 - \hat{a}\Gamma_1)]}{\Gamma_1(1 - \hat{a}\Gamma_1)}\,\frac{d\Gamma_1}{dt}$$

and

$$\frac{d\Gamma_1}{dt} = \frac{k_m(C_b - c_s)}{1 + K_2 c_s \hat{a}\left(\frac{1 + (1 - \hat{a}\Gamma_1)(\hat{a} + \lambda\Gamma_1)}{1 - \hat{a}\Gamma_1}\right)}$$

Here k_m is the mass transfer coefficient and can be evaluated from correlations given elsewhere (27), and the values for parameters $\hat{a}$, K_1, K_2, and λ for BSA and β-casein are given by Guzman et al. (16).

An overall balance for liquid around the foam column gives

$$F = \frac{G\epsilon_T}{1 - \epsilon_T} + B \tag{56}$$

The overall protein balance yields

$$Fc_f = \frac{G\epsilon_T c_d}{1 - \epsilon_T} + Bc_b \tag{57}$$

The pool concentration used in the evaluation of Γ_{pool} in Eq. (51) should satisfy the overall balance Eq. (57).

In order to proceed with the calculations, a liquid pool concentration lower than the feed concentration was assumed. This was used to calculate the kinetics of adsorption of proteins during the formation of the bubbles and their flight in the liquid pool. At the foam–liquid interface, the concentration of proteins in the film is taken to be equal to the pool concentration, and the adsorption of proteins in the liquid pool is evaluated. The concentration of proteins in the top product is evaluated using Eq. (4), and the top product flow rate is evaluated using Eq. (6). From the overall mass balance Eqs. (56) and (57), the pool concentration is calculated. If this calculated concentration agrees well with the assumed concentration, then the program exits. If not, then the pool concentration obtained from the mass balance is used for the second iteration and the calculations are repeated till the assumed and calculated pool concentrations are within the specified error.

EFFECT OF PARAMETERS ON PROTEIN ENRICHMENT AND RECOVERY IN A CONTINUOUS FOAM COLUMN

In order to proceed with the simulations it is necessary to know the feed concentration and flow rates, the gas velocity, the capillary diameter, the capillary constant, the pool height, the foam height, the coalescence frequency, the net charge of the protein molecule, and the ionic strength

of the solution. Once these parameters are known, an iterative solution to the balance equations is obtained as discussed here.

A value for pool concentration is assumed based on the feed concentration. The time of formation of bubbles can be evaluated from the final bubble volume and gas flow rate, whereas the residence time of bubbles in the liquid pool is evaluated from Eq. (54). The surface concentrations of proteins at the end of bubble formation and at the top of liquid pool are evaluated using Eqs. (52) and (51), respectively. The bubble size is evaluated using appropriate equations for bubble formation (26). The film thickness and the area of the Plateau border at the foam–liquid interface are obtained from knowledge of the gas velocity and the bubble size using Eqs. (44)–(48). Coupled partial differential equations (9), (10), (11a), (38), and (39) are solved using the IMSL differential-equation-solving package IVPAG in double precision, employing Gear's method to obtain the profiles of film thickness, area of Plateau border, bubble size, surface concentration of protein, and the bulk concentration of protein in films and Plateau borders along the foam height. The boundary conditions used to solve these equations are given by Eqs. (44)–(47), (49), and (50). The surface concentration of protein at the films is updated using Eq. (36). The liquid holdup is evaluated using Eq. (5). The top product flow rate and protein concentration in the top product are obtained from Eqs. (6) and (4), respectively. From the mass balance (Eqs. 56 and 57), the bottom flow rate and liquid pool concentration are then evaluated. If the relative error between the assumed pool concentration and the calculated value is less than 5%, then enrichment and recovery are calculated using Eqs. (1) and (2), respectively. If the agreement between the assumed and calculated bottoms concentration is not good, the calculated value of the bottoms concentration is taken to be the value of the pool concentration for the next iteration and all the values are set to the initial values. The calculations are repeated until two successive values of pool concentration are within the error bound.

In this section the effect of various operating parameters on the performance of continuous foam fractionation column for BSA are discussed. The ranges of parameters used in calculations are given in Table 1.

Typical variation of enrichment and recovery of BSA with liquid pool height is shown by solid lines in Fig. 2. As can be seen from the figure, enrichment and recovery increase as the liquid pool height increases and eventually attain constant values. The dependence of enrichment on pool height indicates the importance of kinetics of protein adsorption on its concentration in a continuous foam fractionation column. As the liquid pool height is increased, the residence time of bubbles in the pool in-

TABLE 1
Range of Parameters Used in Calculations

Parameter	Range
Bubble size (m)	8×10^{-4} to 2×10^{-3}
Feed concentration (wt%)	0.01–0.6
$\beta\theta$	0–2
Pool height (m)	0–0.3
Feed flow rate (m/s)	2×10^{-5} to 1×10^{-4}
Superficial gas velocity (m/s)	8×10^{-4} to 5×10^{-3}

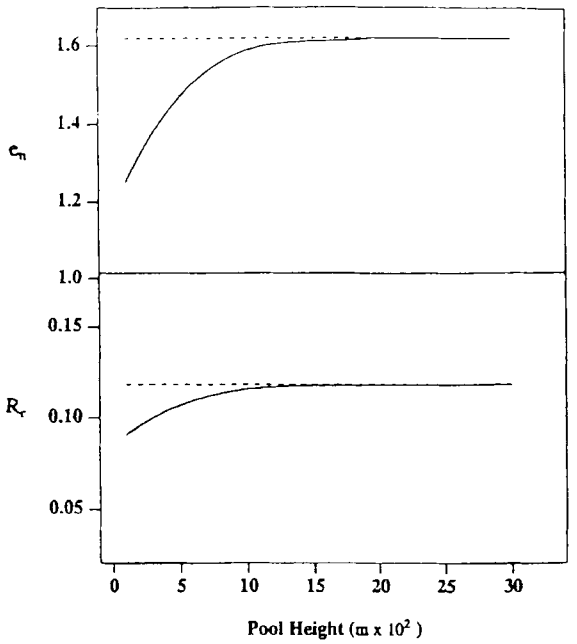

FIG. 2 Effect of kinetics of adsorption of BSA on its enrichment and recovery (solid line). Feed concentration 0.1 wt%, foam height 0.13 m, bubble size 1.6×10^{-3} m, gas velocity 2.6×10^{-3} m/s, feed flow rate 10^{-3} m/s, pH 4.8, and ionic strength 0.1 M. The dashed line shows e_n and R_r when the effect of kinetics of adsorption is neglected.

creases. Because proteins are large molecules, their rate of adsorption is slow compared to small molecular weight surfactants. Consequently, more protein is adsorbed at the gas–liquid interface at a larger residence time of the bubbles, eventually attaining adsorption equilibrium. As a result, the protein enrichment and recovery increase with an increase in the pool height, eventually reaching a constant value. The calculated values of enrichment and recovery at sufficiently large pool heights asymptotically approach the corresponding values for adsorption equilibrium, indicated by the dashed lines in Fig. 2.

Figure 3 shows that as the gas velocity increases, the enrichment decreases whereas the recovery increases. Enrichment is directly proportional to Γ and inversely proportional to ϵ, whereas recovery increases with Γ and ϵ. As can be seen from the inset, the liquid holdup in the foam increases with the gas velocity, leading to lower enrichment and higher

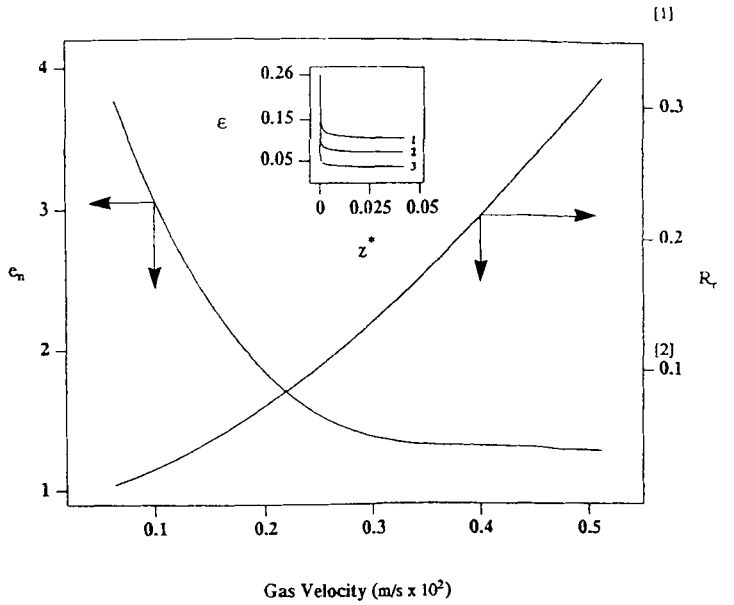

FIG. 3 Effect of gas velocity on enrichment and recovery of BSA. Bubble size 9×10^{-4} m, foam height 0.13 m, liquid pool height 0.24 m, feed flow rate 10^{-3} m/s, feed concentration 0.1 wt%, pH 4.8, and ionic strength 0.1 M. Inset shows the variation of ϵ at different gas velocities and liquid holdup along dimensionless foam height for different gas velocities. Gas velocities are 3.8×10^{-3}, 2.5×10^{-3}, and 1.3×10^{-3} m/s for Curves 1, 2, and 3, respectively.

recovery. Consequently, there would be an optimum gas velocity at which protein enrichment and recovery would have desirable values.

The effect of kinetics of adsorption on enrichment and recovery for different gas velocities is shown in Fig. 4. As the liquid pool height increases, the residence time of bubbles in the pool increases, leading to higher surface concentration of protein on bubbles. This leads to an increase in enrichment with liquid pool height. Once the surface concentration of proteins on bubbles is equal to the equilibrium concentration, there is no further increase in Γ and hence enrichment, and recovery takes place. Further, enrichment over the entire range of pool height is lower for higher gas velocity owing to the increase in liquid holdup. The recovery, on the other hand, is higher for higher gas velocity because the liquid holdup would be higher. Consequently, there would be an optimum gas velocity at which protein enrichment and recovery would have desirable values.

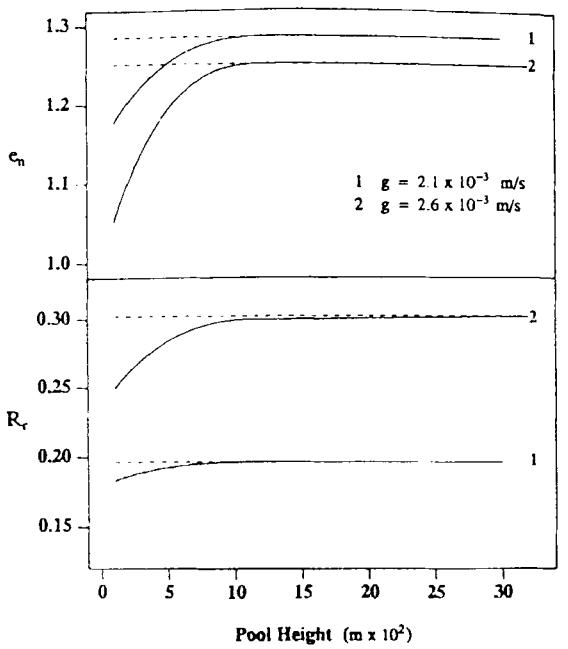

FIG. 4 Effect of kinetics of adsorption on enrichment and recovery of BSA. Feed concentration 0.1 wt%, foam height 0.13 m, bubble size 9×10^{-4} m, gas velocity 2.6×10^{-3} m/s, feed flow rate 1.71×10^{-3} m/s, pH 4.8, and ionic strength 0.1 M. The dashed lines indicate the e_n and R_r when the effect of kinetics of adsorption is neglected.

As depicted in Fig. 5, the liquid holdup decreases with an increase in the bubble size. The drainage of liquid depends on the initial distribution of liquid in films and Plateau borders. The films drain much faster than the Plateau borders. As the bubble size increases, the fraction of liquid in the film increases, thus resulting in faster liquid drainage from the foam. Thus the liquid holdup decreases with an increase in the bubble size. Figure 6 shows the effect of bubble size on enrichment and recovery. Bubble size determines the residence time of bubbles in the liquid pool and the mass transfer coefficient for adsorption of protein in the liquid pool. The residence time and mass transfer coefficient are more for smaller bubbles. This would tend to increase the surface concentration of protein. In addition, smaller bubbles give rise to higher interfacial area per unit volume of the foam and hence higher enrichment and recovery. Smaller bubbles also lead to higher liquid holdup (see Fig. 5), which tends to decrease enrichment. Thus, the bubble size plays an important role in determining enrichment. Depending on the effect that dominates, the enrichment and recovery would either increase or decrease with bubble size. There would, therefore, exist an optimum bubble size for maximum enrichment (1). For the bubbles sizes in the range of 0.07 to 0.2 mm, it was found that as the bubble size increases, the enrichment increases, and the recovery of proteins decreases.

To demonstrate the feasibility of foam concentration as a useful technique for separating proteins from very dilute streams, calculations were done to show the effect of feed concentration on enrichment and recovery.

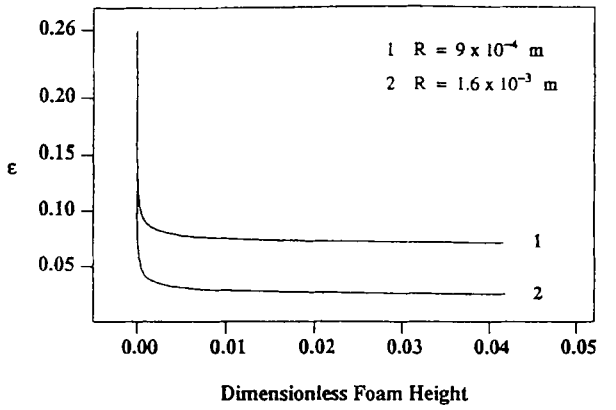

FIG. 5 Effect of bubble size on liquid holdup profile in a foam column; feed concentration 0.1 wt% BSA, liquid pool height 0.24 m, foam height 0.13 m, gas velocity 2.1×10^{-3} m/s, feed flow rate 1.71×10^{-2} m/s, pH 4.8, and ionic strength 0.1 M.

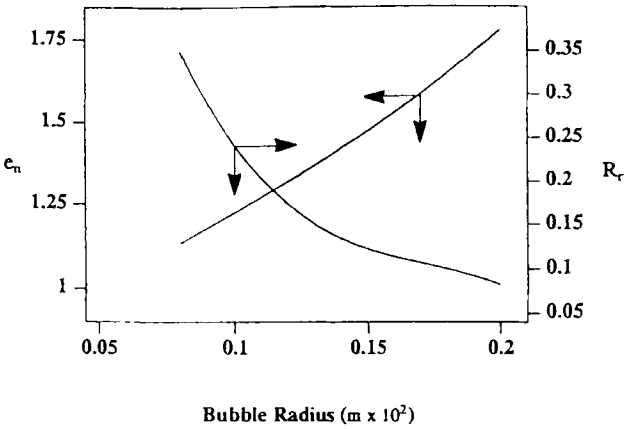

FIG. 6 Effect of bubble radius on enrichment and recovery of BSA. Feed concentration 0.1 wt%, pool height 0.24 m, foam height 0.13 m, feed flow rate 10^{-3} m/s, gas velocity 2.1 $\times$ 10^{-3} m/s, pH 4.8, and ionic strength 0.1 M.

These results are shown in Fig. 7. As can be seen from the figure, the enrichment and recovery are high at lower feed concentration, and they decrease rapidly as the concentration of protein in the feed increases. At low protein concentrations, less protein is adsorbed at the gas–liquid interface. However, the contribution of adsorbed protein to enrichment increases since the amount of protein in the bulk is smaller. The latter effect predominates at lower protein concentration so that the enrichment increases.

The effect of feed flow rate on enrichment and recovery is shown in Fig. 8. Enrichment increases, whereas recovery decreases, with an increase in the feed flow rate. At low feed flow rates, the residence time of the liquid in the pool is large. As a result, the pool concentration is lower than the feed concentration. This results in lower rates of protein adsorption and hence smaller enrichment. On the other hand, for high feed flow rates, the residence time of liquid in the pool is small. Consequently, the pool concentration is close to the feed concentration. Recovery, on the other hand, decreases with an increase in the feed flow rate because the total protein entering the foam column increases.

In the above calculations it is assumed that the bubble size does not change in the foam column. Experimental observations of bubble size indicate that bubble size increases with foam height due to coalescence (28). The coalescence frequency of bubbles can be evaluated from knowledge of variation of bubble size along the foam height. Here, computations

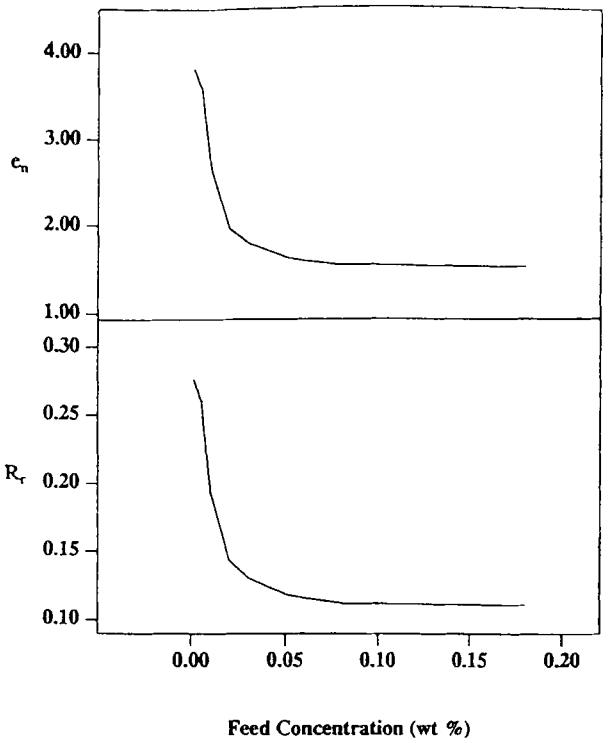

FIG. 7 Effect of feed concentration on enrichment and recovery of BSA. Liquid pool height 0.24 m, foam height 0.13 m, gas velocity 2.1×10^{-3} m/s, bubble size 9×10^{-4} m, feed flow rate 10^{-3} m/s, pH 4.8, and ionic strength 0.1 M.

are done by assuming various models of coalescence frequencies to show their effect on the performance of the foam column. These calculations consider coalescence of bubbles only in the foam. Consequently, bubbles are assumed not to undergo any coalescence during their flight in the liquid pool.

Calculations were done at a constant coalescence frequency to show the effect of bubble coalescence on bubble size, number of bubbles per unit volume, and liquid holdup along the foam height. The results for two coalescence frequencies are shown in Fig. 9. For low values of β, the bubble size, N and ϵ do not change very much along the foam height. On the other hand, for high coalescence frequency β, the bubble size increases more rapidly along the foam height. As a result, the number of bubbles per unit volume decreases with foam height. Because of increased liquid

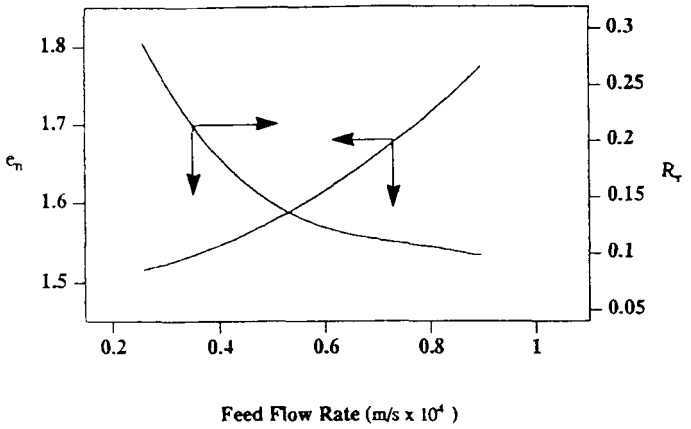

FIG. 8 Effect of feed flow rate on enrichment and recovery of BSA. Feed concentration 0.1 wt%, liquid pool height 0.24 m, foam height 0.13 m, gas velocity 2.1 × 10^{-3} m/s, pH 4.8, and ionic strength 0.1 M.

drainage due to larger bubble sizes, the liquid holdup is found to decrease faster along the foam height.

The effect of dimensionless coalescence frequency $\beta\theta$ (where θ is the residence time of bubbles in foam) on enrichment and recovery for two bubble sizes is shown in Fig. 10. Enrichment increases with an increase in $\beta\theta$, whereas the recovery decreases. Moreover, the bubble size increases more rapidly with coalescence frequency for larger bubbles than for smaller bubbles, thus resulting in stronger dependence of enrichment and recovery on coalescence for larger bubbles. Coalescence leads to 1) an increase in the protein concentration due to internal reflux with subsequent increase in the surface concentration due to faster rates of adsorption, 2) a decrease in the liquid holdup because of increased liquid drainage rates as a result of larger bubble sizes, and 3) a decrease in the surface area because of larger bubble sizes. The first two effects lead to an increase in the enrichment whereas the last two effects lead to lower recoveries. The second effect seems to be predominant since coalescence leads to higher enrichment and lower recovery, as can be seen from Fig. 10.

In the results discussed above, it was assumed that the coalescence frequency is constant. In reality, the coalescence frequency would depend on the bubble size. Comparison of the predicted enrichment and recovery for three different models for coalescence is shown in Fig. 11, where the

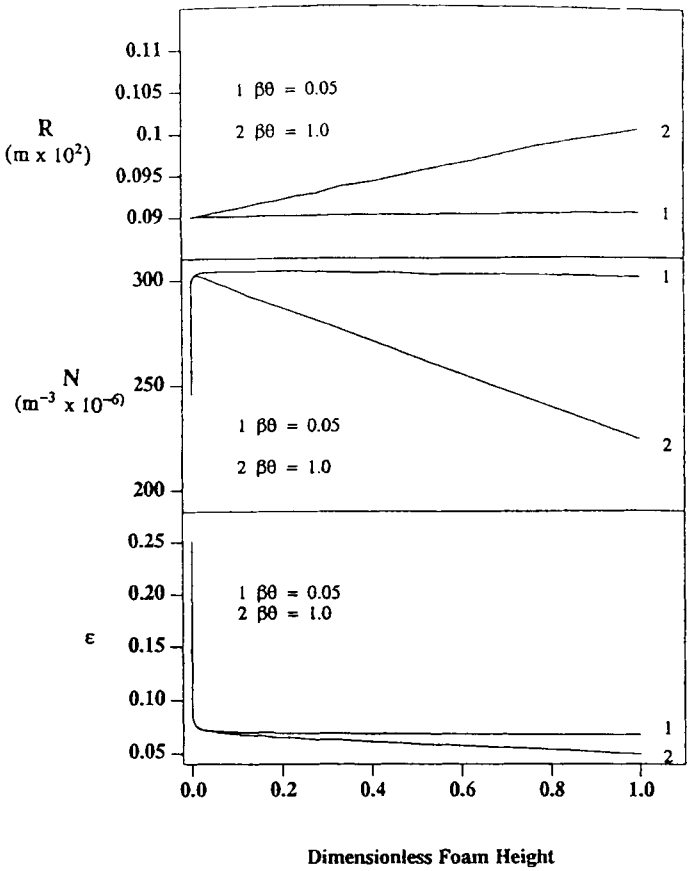

FIG. 9 Effect of change in R, N, and ϵ along dimensionless foam height for two coalescence frequencies; feed concentration 0.1 wt%, pool height 0.24 m, foam height 0.13 m, gas velocity 2.6×10^{-3} m/s, inlet bubble size 9×10^{-4} m, pH 4.8, and ionic strength 0.1 M.

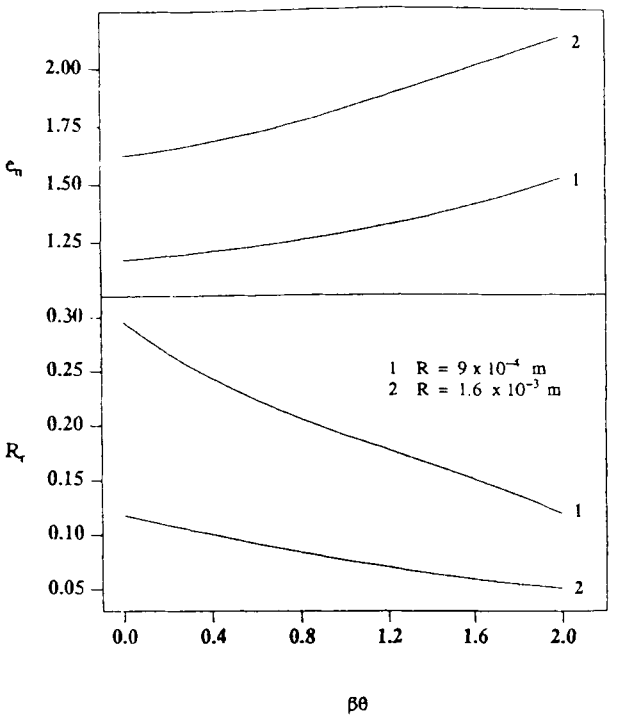

FIG. 10 Effect of dimensionless coalescence frequency on enrichment and recovery of BSA for different bubble sizes. Feed concentration 0.1 wt%, liquid pool height 0.24 m, foam height 0.13 m, bubble size 9×10^{-4} m, gas velocity 2.6×10^{-3} m/s, feed flow rate 10^{-3} m/s, pH 4.8, and ionic strength 0.1 M.

enrichment and recovery are plotted for different values of $\beta_0\theta$, where β_0 is the coalescence frequency corresponding to the inlet bubble size. Enrichment is the highest and recovery lowest for the model in which $\beta \propto R^2$. Enrichments were found to decrease in the order $\beta \propto R^2 > \beta \propto R > \beta = \beta_0$. Such a behavior is to be expected since the coalescence frequency decreases in the same order. At very low coalescence frequencies, however, there was very little difference in the enrichments and recoveries predicted by the models. As pointed out earlier, the protein enrichment

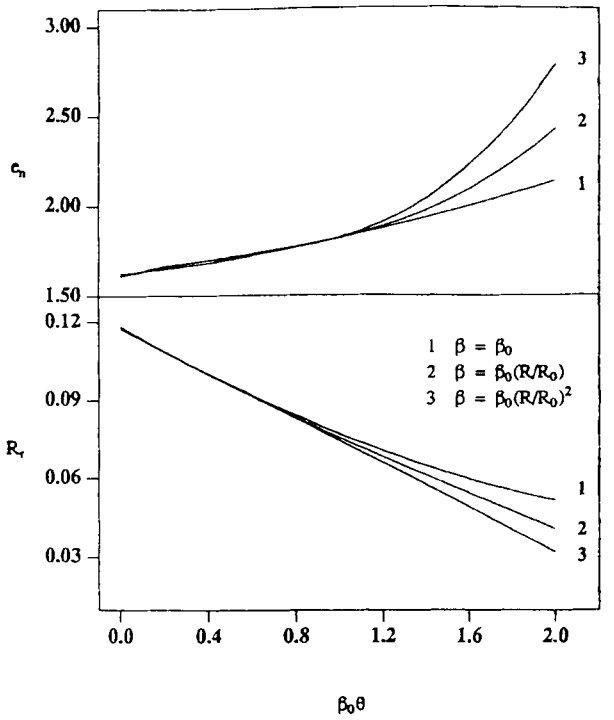

FIG. 11 Comparison of predicted enrichment and recovery for three models of coalescence frequency. Feed concentration 0.1 wt%, pool height 0.24 m, foam height 0.13 m, bubble size 9×10^{-4} m, gas velocity 2.6×10^{-3} m/s, feed flow rate 10^{-3} m/s, pH 4.8, and ionic strength 0.1 M.

is higher and the recovery lower for higher coalescence frequencies because of 1) lower liquid holdup as a result of increased liquid drainage due to larger bubbles, and 2) more adsorption of proteins because of higher bulk concentration resulting from internal reflux.

CONCLUSIONS

A model for the hydrodynamics of a continuous foam column for the concentration of proteins was proposed. This model accounts for the ki-

netics of adsorption of proteins during the formation of bubbles as well as the flight of bubbles in the liquid pool and in foam. Drainage of thin films under Plateau border suction and disjoining pressure due to van der Waals attraction and double-layer repulsion were accounted for in this model. In calculating the velocity of drainage of films, the surface of the films was considered to be immobile whereas the surface viscosity was accounted for in the evaluation of the drainage of liquid from Plateau borders. Plateau borders were considered to be randomly oriented in the foam bed, and the drainage of Plateau borders was considered in the evaluation of liquid holdup in the foam. Bubble sizes at any cross section of the foam bed were considered to be uniform, though the variation of bubble sizes along the foam height was accounted for through a dimensionless coalescence frequency.

According to the model for the foam bed, the liquid holdup decreases rapidly near the foam–liquid interface and changes slowly along the height of the foam column. Increasing the gas velocity leads to higher liquid holdup whereas increasing bubble size results in lower liquid holdup in the foam. The model is able to predict the effect of kinetics of adsorption of protein on the enrichment and recovery of proteins. As the liquid pool height was increased, the enrichment and recovery increased and leveled off at the pool height where the concentration of proteins at the gas–liquid interface reached equilibrium value. It was found that as the gas velocity was increased, the enrichment decreased whereas the recovery increased. The effect of increase in bubble size was to increase the enrichment and decrease the recovery. Further, increasing the feed concentration led to lower enrichment and recovery, implying that the technique of foam fractionation is most attractive at lower feed concentrations. The enrichment increased with an increase in the feed flow rate whereas the recovery decreased as the feed flow rate was increased. In the case where coalescence of foam was accounted for, the enrichment increased with an increase in dimensionless coalescence frequency whereas the recovery decreased. The bubble sizes increase more rapidly with coalescence frequency for larger bubbles than for smaller bubbles, thus resulting in a stronger dependence of enrichment and recovery for larger bubble sizes.

SYMBOLS

a_p	cross-sectional area of the Plateau border (m^2)
A_p	projected area of the bubble (m^2)
$\hat{a}$	average surface area occupied by an adsorbed protein molecule ($m^2 \times 10^6$/kg)
A_f	area of film (m^2)

A_F	flow unit area (m^2)
B	bottoms flow rate per unit column cross-sectional area (m/s)
c_b	bulk protein concentration (kg/m^3)
c_p	protein concentration in plateau borders (kg/m^3)
c^*	dimensionless concentration of proteins in subsurface ($= c_s/c_{pool}$)
c_v	velocity coefficient for gravity drainage of Plateau border
c_s	bulk protein concentration in equilibrium with surface concentration Γ (kg/m^3)
c_f	concentration of proteins in film (kg/m^3)
C_D	drag coefficient in Eq. (53)
c_T	protein concentration in top product (kg/m^3)
c_F	protein concentration in feed (kg/m^3)
c_{pool}	protein concentration in the liquid pool (kg/m^3)
D	diffusion coefficient (m^2/s)
d_f	final diameter of the bubble (m)
e	electronic charge (1.602×10^{-19} C)
e_n	enrichment factor
F_t	feed flow rate of top product per unit column cross-sectional area (m/s)
F	feed flow rate per unit column cross-sectional area (m/s)
g	acceleration due to gravity (m/s^2)
G	superficial gas velocity (m/s)
h	Planck's constant (6.6242×10^{-34} J·s)
k	Boltzmann's constant (1.38×10^{-34} J/K)
k_m	mass transfer coefficient
K_1	rate constants for monolayer adsorption of protein (wt%)
K_2	rate constants for multilayer adsorption of protein (kg $\times 10^{-6}/m^2$·wt%)
l	length of Plateau border (m) ($= 0.816R$)
L_{pool}	height of the liquid pool (m)
n_f	number of films per bubble
n_p	number of Plateau borders per bubble
n_p'	number of Plateau borders per bubble on a horizontal plane
N	number of bubbles per unit volume of the foam bed (m^{-3})

p	pressure (N/m^2)
p^*	dimensionless pressure as defined by Eq. (22)
Pe	Peclet number, $V_f x_f/D$
q	charge on the protein molecule
Q_E	flow rate at the end of the expansion stage (m^3/s)
Q_f	flow rate of gas through capillary (m^3/s)
r^*	dimensionless radial distance from the center of the film ($= r/R_F$)
R_r	recovery of protein
R	radius of bubbles (m)
R^*	dimensionless radius of bubbles ($= R/R_0$)
R_0	bubble radius at gas liquid interface (m)
R_F	film radius (m)
R_p	radius of the Plateau borders (m)
S	dimensionless group used in Eq. (21), $= (\Delta P x_f)/(\partial \pi_s/\partial \Gamma)_{\bar{\Gamma}}$
T	absolute temperature (K)
$t_{formation}$	time of formation of bubbles (s)
t^*	dimensionless time, Eq. (33) ($= tV_f/x_f$)
x_f	film thickness (m)
v_b	volume of the foam bubble (m^3)
V_f	velocity of drainage of films (m/s)
u	velocity of drainage of Plateau borders (m/s)
u_{pool}	velocity of the bubble in the liquid pool (m/s)
v_z	axial component of velocity of drainage of film (m/s)
v_r	radial component of velocity of drainage of film (m/s)
v_z^*	dimensionless axial component of velocity of drainage of film ($= v_z/V_f$)
v_r^*	dimensionless radial component of velocity of drainage of film (v_r/V_f)
z	axial distance from the foam liquid interface (m)
z^*	dimensionless axial distance in the film ($= z/x_f$)

Subscripts

T	top
O	foam–liquid interface

Greek Symbols

ϵ	liquid holdup in the foam
ϵ_T	liquid holdup in the foam at the top of column

η	flow of number of bubbles in foam per unit area and unit time ($m^{-2} \cdot s^{-1}$)
β	coalescence frequency, fraction of bubbles coalescing per unit time (s^{-1})
ΔP	pressure drop between films and Plateau borders (N/m^2)
σ	surface tension (N/m)
σ_s	surface charge density
Π_{VW}	disjoining pressure due to van der Waal's interactions (N/m^2)
Π_{DW}	disjoining pressure due to electrostatic interactions interactions (N/m^2)
π_s	surface pressure due to interfacial protein layer (N/m)
σ_0	surface tension of pure water (N/m)
λ	constant ($m^2 \times 10^6/kg$)
Γ	surface concentration of proteins (kg/m^2)
Γ'	number concentration of proteins ($number/m^2$)
Γ^*	dimensionless surface concentration ($= \Gamma/\Gamma_0$)
$\bar{\Gamma}$	average surface concentration of protein in films (kg/m^2)
Γ_1	surface concentration in the first layer of adsorption (kg/m^2)
Γ_2	surface concentration in the second layer of adsorption (kg/m^2)
γ_f	inverse dimensionless surface viscosity for films
μ_s	surface viscosity of the film interface
μ	viscosity
ΔG	activation energy for flow
Γ_0	surface concentration of protein at the foam–liquid interface (kg/m^2)
Φ_{F0}	fraction of liquid present in the film
$\Gamma_{formation}$	surface concentration on bubble at the end of the formation step (kg/m^2)
Γ_{pool}	surface concentration on bubble at the top of the liquid pool (kg/m^2)
θ	residence time of bubble in the liquid pool (s)
ρ	density of aqueous phase (kg/m^3)
$(d\Gamma/dt)_f$	rate of protein adsorption in films
$(d\Gamma/dt)_{formation}$	rate of protein adsorption during bubble formation
$(d\Gamma/dt)_{pool}$	rate of protein adsorption on bubble in the liquid pool

ACKNOWLEDGMENT

We acknowledge the National Science Foundation (Grant BCS-91-12154) for partial support of this work.

REFERENCES

1. G. Narsimhan and E. Ruckenstein, "Hydrodynamics, Enrichment and Collapse in Foams," *Langmuir*, *2*, 230 (1986).
2. G. D. Miles, L. Shedlovsky, and J. Ross, "Foam Drainage," *J. Phys. Chem.*, *49*, 93 (1945).
3. W. M. Jacobi, K. E. Woodcock, and C. S. Grove, "Theoretical Investigation of Foam Drainage," *Ind. Eng. Chem.*, *48*, 2046 (1956).
4. S. Hartland and A. D. Barber, "A Model for a Cellular Foam," *Trans. Inst. Chem. Eng.*, *52*, 43 (1974).
5. L. Steiner, R. Hunkeler, and S. Hartland, "Behavior of Dynamic Cellular Foams," *Ibid.*, *55*, 153 (1977).
6. D. Desai and R. Kumar, "Flow through a Plateau Border of Cellular Foam," *Chem. Eng. Sci.*, *37*, 1361 (1982).
7. D. Desai and R. Kumar, "Liquid Holdup in Semi-batch Cellular Foams," *Ibid.*, *38*, 1525 (1983).
8. D. Desai and R. Kumar, "Liquid Overflow from Vertical Cocurrent Foam Columns," *Ibid.*, *39*, 1559 (1984).
9. R. Lemlich, "Prediction of Changes in Bubble Size Distribution Due to Interbubble Gas Diffusion in Foams," *Ind. Eng. Chem. Fundam.*, *17*, 89 (1978).
10. A. Monsalve and R. S. Schechter, "The Stability of Foams: Dependence of Observation on the Bubble Size Distribution," *J. Colloid Interface Sci.*, *97*(2), 327 (1984).
11. I. C. Callaghan, F. T. Lawrence, and P. M. Melton, "An Equation Describing Aqueous and Nonaqueous Foam Collapse," *Colloid Polym. Sci.*, *268*, 423 (1986).
12. V. V. Krotov, "Hydrodynamic Stability of Polyhedral Disperse Systems and Their Kinetics under Conditions of Spontaneous Breakdown. 2. Capillary Stability of Disperse Phase," *Kolloidn. Zh.*, *48*, 913 (1984).
13. V. V. Krotov, "Hydrodynamic Stability of Polyhedral Disperse Systems and Their Kinetics under Conditions of Spontaneous Breakdown. 3. Kinetics Associated with Film Instability," *Ibid.*, *48*, 1170 (1984).
14. G. Narsimhan and E. Ruckenstein, "Effect of Bubble Size Distribution on the Enrichment and Collapse in Foams," *Langmuir*, *2*, 494 (1986).
15. L. K. Brown, G. Narsimhan, and P. C. Wankat, "Foam Fractionation of Globular Proteins," *Biotechnol. Bioeng.*, *36*, 947 (1990).
16. R. Z. Guzman, R. G. Carbonell, and P. K. Kilpatrick, "The Adsorption of Proteins at Gas–Liquid Interface," *J. Colloid Interface Sci.*, *114*, 536 (1986).
17. G. Narsimhan and F. Uraizee, "Kinetics of Adsorption of Globular Proteins at an Air–Water Interface," *Biotechnol. Prog.*, *8*, 187 (1992).
18. R. Kumar and N. R. Kuloor, "The Formation of Bubbles and Drops," *Adv. Chem. Eng.*, *8*, 255 (1970).
19. F. A. Uraizee and G. Narsimhan, "Surface Equation of State for Globular Proteins in the Air–Water Interface," *J. Colloid Interface Sci.*, *146*, 169 (1989).
20. R. A. Leonard and R. Lemlich, "A Study of Interstitial Liquid Flow in Foam. Part I. Theoretical Model and Applications to Foam Fractionation," *AIChE J.*, *11*, 18 (1965).

21. J. Gregory, "Approximate Expression for Retarded van der Waals Interactions," *J. Colloid Interface Sci.*, *83*, 138 (1981).
22. R. J. Hunter, *Foundations of Colloid Science*, Oxford University Press, New York, 1987.
23. W. J. Moore and H. Eyring, "Theory of Viscosity of Unimolecular Films," *J. Chem. Phys.*, *6*, 391 (1938).
24. D. E. Graham and M. C. Phillips, "Proteins at Liquid Interfaces. V. Shear Properties," *J. Colloid Interface Sci.*, *76*, 240 (1980).
25. A. Satyanarayan, R. Kumar, and N. R. Kuloor, "Studies in Bubble Formation. I. Bubble Formation under Constant Pressure Conditions," *Chem. Eng. Sci.*, *24*, 749 (1969).
26. A. T. Popovich, R. E. Jervis, and O. Trass, "Mass Transfer during Single Bubble Formation," *Ibid.*, *19*, 357 (1964).
27. R. Clift, J. R. Grace, and M. E. Weber, *Bubbles, Drops and Particles*, Academic Press, New York, 1978.
28. F. A. Uraizee, "Effects of Kinetics of Adsorption and Coalescence on Continuous Foam Concentration of Proteins," Ph.D. Thesis, Purdue University, West Lafayette, Indiana, USA, 1991.

Received by editor August 15, 1994